Ophthalmol Ther (2025) 14:2395–2413
https://doi.org/10.1007/s40123-025-01210-2

ORIGINAL RESEARCH

One-Month Changes in Choroidal Vascularity Index of Medium Vessel Layer in Children with Myopia Wearing Orthokeratology Lenses: a Predictor for One-Year Changes in Axial Length

Junmeng Li · Bei Rong · Lei Zhu · Ruilin Zhu · Xin Rong · Yuwei Wang · Yadi Zhang · Xiaopeng Gu · Shuang Zeng · Yanye Lu · Liu Yang

Received: June 10, 2025 / Accepted: July 10, 2025 / Published online: July 30, 2025
© The Author(s) 2025

ABSTRACT

***Introduction*:** Orthokeratology (ortho-K) is an established intervention for myopia control in children, yet the vascular mechanisms within the choroidal sublayers underlying its efficacy remain unclear. This study aims to investigate the changes in the choroidal vascularity index (CVI) of choroid sublayers after ortho-K treatment, the association between 1-month CVI changes and 1-year axial length (AL) elongation, and the role of CVI responses in predicting the 1-year control efficacy of ortho-K treatment.

***Methods*:** A prospective cohort study was conducted, enrolling 257 children with myopia aged 7–16 years. The subjects wore ortho-K lenses continuously for 12 months. Choroidal volume, vascular volume (CVV), stromal volume (CSV), and CVI of the choroid sublayers were assessed using optical coherence tomography images at baseline and 1-month follow-up. The total choroidal layer (TCL) includes the large-vessel choroidal layer (LVCL) and the medium-vessel choroidal layer (MVCL). The Early Treatment of Diabetic Retinopathy Study (ETDRS) grid divides the macular area into nine subfields for detailed analysis.

***Results*:** The 1-month CVI of TCL and MVCL in all ETDRS grid regions were significantly lower than the baseline CVI ($P \leq 0.036$), except for the superior outer ring subfield in TCL ($P = 0.070$). After the 1-month ortho-K treatment, both choroidal volume and CSV significantly increased in all choroidal sublayers compared with baseline data ($P \leq 0.027$), while CVV also showed significant increases in half of the ETDRS grid regions (14/27). After adjusting for age and gender, the baseline CVI of temporal inner ring subfield in TCL ($\beta = 0.146$, $P = 0.006$), and 1-month CVI changes of the temporal outer ring subfield ($\beta = 0.337$, $P < 0.001$) and nasal inner ring subfield ($\beta = 0.174$, $P = 0.002$) in MVCL, were independently associated with 1-year AL elongation during ortho-K treatment. On the basis of the 1-month CVI changes

Supplementary Information The online version contains supplementary material available at https://doi.org/10.1007/s40123-025-01210-2.

J. Li · B. Rong · R. Zhu · X. Rong · Y. Wang · Y. Zhang · X. Gu · L. Yang (✉)
Department of Ophthalmology, Peking University First Hospital, No. 8 Xi Shi Ku Street, Xicheng District, Beijing 100034, China
e-mail: liu_yang@bjmu.edu.cn

L. Zhu · S. Zeng · Y. Lu
Institute of Medical Technology, Peking University Health Science Center, Peking University, No. 38 Xueyuan Road, Haidian District, Beijing 100191, China

L. Zhu · S. Zeng
Department of Biomedical Engineering, College of Future Technology, Peking University, No.5 Yiheyuan Road, Haidian District, Beijing 100871, China

of temporal outer ring subfield and nasal inner ring subfield in MVCL, as well as age and sex, the prediction model demonstrated an area under the curve (AUC) of 0.905 (95% CI 0.870–0.941) for distinguishing children with myopia who exhibited slow versus fast AL elongation.

Conclusions: After the 1-month ortho-K treatment, choroidal volume, CVV, and CSV, of all choroidal sublayers significantly increased, while CVI of TCL and MVCL significantly decreased. The CVI in LVCL showed no significant changes. The differences in short-term CVI changes among choroidal sublayers indicate disproportionate changes in CVV and CSV, which help to explore the possible choroidal mechanisms of myopia control with ortho-K treatment. Early CVI changes in MVCL possess potential clinical significance for predicting long-term AL elongation.

Keywords: Myopia; Orthokeratology; Choroidal vascularity index; Axial length; Predictor

Key Summary Points

Why carry out this study?
Orthokeratology (ortho-K) is a widely used intervention for myopia control in children, but the choroidal vascular mechanisms underlying its efficacy remain unclear
This study aimed to determine how choroidal vascularity indices (CVI) of sublayers change after ortho-K treatment and whether early CVI alterations predict long-term axial elongation outcomes
Short-term CVI changes in choroidal sublayers following ortho-K treatment are associated with and predictive of 1-year axial length control efficacy

What has been learned from the study?
After 1 month of Ortho-K treatment, vascular and stromal volumes increased across choroidal sublayers; however, CVI decreased in the total and medium-vessel layers, suggesting disproportionate remodeling. Early CVI changes in specific regions independently predicted 1-year axial elongation (AUC 0.905)
Disparate CVI responses among choroidal sublayers highlight potential mechanisms of myopia control through vascular–stromal balance modulation
Monitoring early CVI changes in medium-vessel choroidal layers may provide a clinically actionable biomarker to identify children likely to benefit from ortho-K

INTRODUCTION

The global prevalence of myopia, particularly in East Asia, is rising at an alarming rate. By 2050, it is projected that the prevalence of myopia and high myopia will encompass approximately 50% and 10% of the global population, respectively [1]. Axial length (AL) elongation associated with myopia development significantly escalates the risk of vision-threatening eye complications, such as myopic macular degeneration and retinal detachment [2]. Therefore, it is crucial to implement interventions that can decelerate myopia progression in children.

Orthokeratology (ortho-K) is regarded as one of the most efficacious optical interventions for controlling myopia. Numerous studies have reported that the rate of AL reduction following ortho-K treatment ranges from 30% to 63% [3–5]. However, some children undergoing ortho-K treatment continue to experience rapid myopia progression. Given that evaluating the treatment effect typically requires a 1-year timeframe, this delay can impede the initiation of timely and effective myopia control measures, thereby inevitably heightening the risk of myopia progression [6].

Multiple studies have investigated demographic and baseline ocular factors influencing the efficacy of myopia control through ortho-K

treatment, including age [3–5, 7–9], spherical equivalent refraction (SER), AL [10–12], and central corneal thickness [7]. However, disparate studies yield conflicting outcomes, particularly regarding baseline SER [4, 13, 14]. Following ortho-K lens use, the relative corneal refraction in the middle-peripheral cornea increases, leading to peripheral retinal myopia defocus and slowing myopia progression [15, 16]. Nonetheless, even when patients wear the same brand of ortho-K lenses, variations in corneal topography and differences in peripheral retinal myopia defocus due to lens parameters can influence the outcome of myopia control. This variability may contribute to the conflicting findings observed in various studies. Therefore, factors that respond rapidly to peripheral retinal myopia defocus following ortho-K treatment may serve as more reliable predictors of myopia control outcomes.

Alterations in choroidal structure may serve as a medium for myopia control after ortho-K treatment. Several studies have reported significant increases in choroidal thickness following short-term ortho-K treatment [16–19], which significantly correlated with AL changes [16, 18, 19]. However, choroidal thickness varies significantly with age, SER, AL, intraocular pressure, and systolic blood pressure [20, 21], and is sensitive to segmentation errors [22]. The choroidal vascularity index (CVI) is derived from the ratio of the lumen area to the choroidal cross-sectional area in a single B-scan image obtained using optical coherence tomography (OCT). Compared with choroidal thickness, CVI offers superior reproducibility, as it is unaffected by age, systolic blood pressure, AL, and intraocular pressure [23, 24]. CVI allows for more reliable and precise assessments of the choroidal vasculature. Recent research has identified short-term CVI changes in children with myopia after ortho-K treatment through calculations on the basis of a single B-scan OCT image [6, 25].

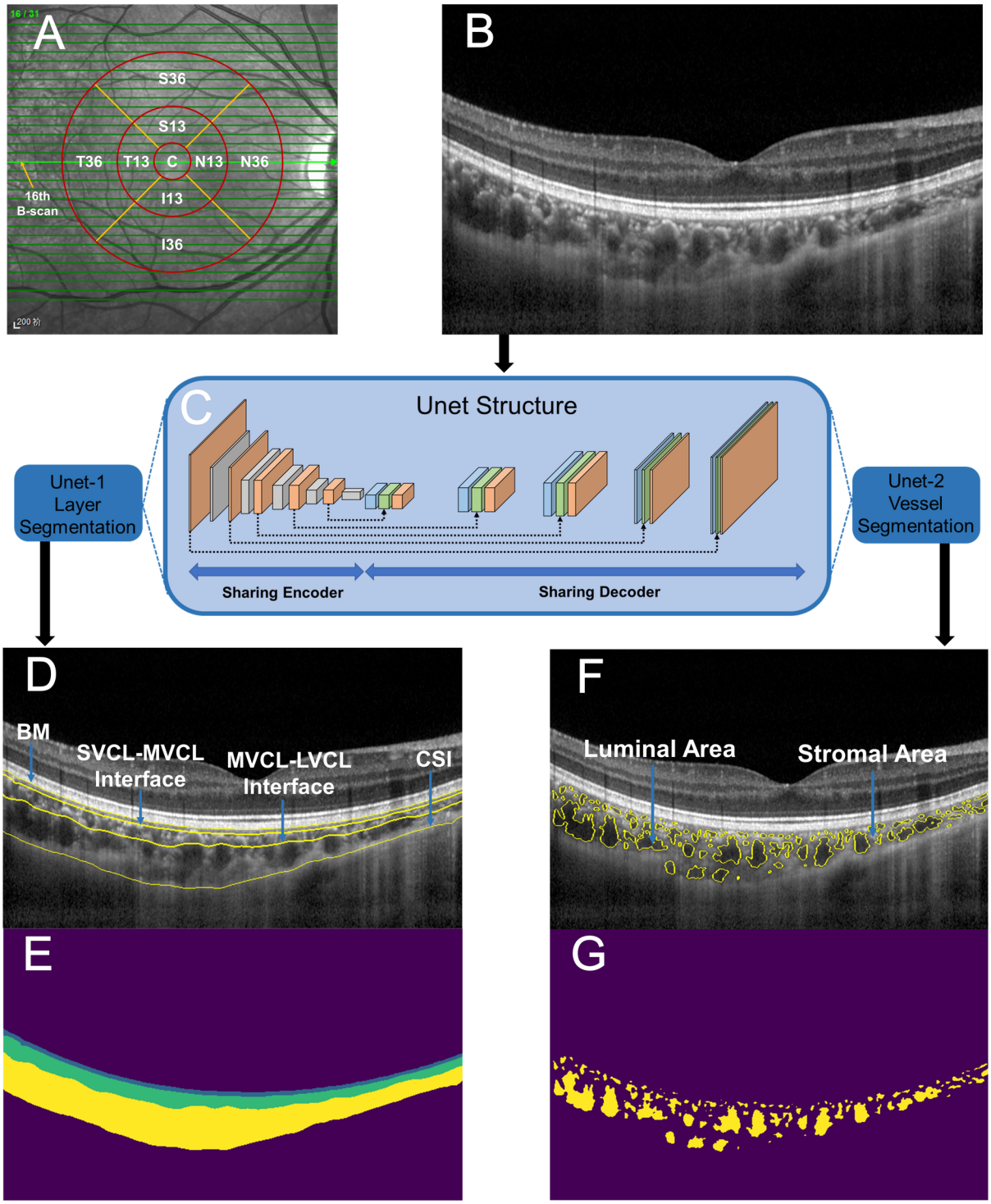
However, CVI calculated from a single B-scan image cannot fully represent the characteristics of the choroidal vasculature. Three-dimensional or volumetric information of the choroid should be utilized for a more accurate evaluation of the choroidal vasculature, rather than relying solely on two-dimensional single B-scan images [26]. Our research group developed an automated choroidal analysis model on the basis of deep learning, capable of calculating the three-dimensional CVI of choroidal sublayers. We observed that the stroma and vessels in choroidal sublayers decreased disproportionately in children with myopia [24]. Li et al. observed significant choroidal thickening after 1-month and 6-month Ortho-K treatments in children with myopia, with the thickening of the large vessel choroidal layer contributing to the majority of this increase [17]. This highlights the potential significance of analyzing the inner structures of choroidal sublayers.

The aim of this study was to investigate the 1-month CVI changes in the total choroid and its sublayers, and their relationship with 1-year AL elongation in children with myopia following ortho-K treatment. Furthermore, we explored the predictive impact of 1-month CVI changes on myopia control efficacy, offering insights for early intervention strategies in myopia control.

METHODS

Subjects

This prospective cohort study adhered to the principles of the Declaration of Helsinki and received approval from the ethical committee of Peking University First Hospital (approval no.: 2022-KY-190-001). Written informed consent was obtained from all participants and their guardians. Subjects were recruited and screened consecutively from October 2021 to November 2022. Children willing to wear ortho-K lenses were enrolled and followed up for 1 year. Inclusion criteria included: age 7–16 years, corrected visual acuity of 20/20 or above, SER between −5.75D and −0.75D, astigmatism ≤ 2.00D, and interocular difference ≤ 1.50D. Exclusion criteria included a history of ocular surface or fundus diseases, or any myopia control methods other than monocular lenses, such as hard contact lenses, multifocal soft contact lenses, and atropine.


A
S36
S13
T36
T13
C
N13
N36
I13
I36
16th
B-scan
B
C
Unet Structure
Unet-1
Layer
Segmentation
Unet-2
Vessel
Segmentation
Sharing Encoder
Sharing Decoder
D
BM
SVCL-MVCL
Interface
MVCL-LVCL
Interface
CSI
E
F
Luminal Area
Stromal Area
G

◂**Fig. 1** Schematic diagram of the ETDRS grid area and the automatic choroidal sublayer segmentation. **A** Near-infrared reflectance image showing the nine subfields in the ETDRS grid, including the central (C), superior inner ring (S13), inferior inner ring (I13), temporal inner ring (T13), nasal inner ring (N13), superior outer ring (S36), temporal outer ring (T36), inferior outer ring (I36), and nasal outer ring (N36). **B** Unsegmented original B-scan image. **C** Unet Structure for choroidal segmentation. **D** and **E** Visualization of choroidal layer segmentation. **F** and **G** Visualization of choroidal vessel segmentation. *ETDRS* Early Treatment of Diabetic Retinopathy Study, *BM* Bruch's membrane, *SVCL* small-vessel choroidal layer, *MVCL* medium-vessel choroidal layer, *LVCL* large-vessel choroidal layer, *CSI* choroidal scleral interface

Following lens dispensing, patients are advised to wear ortho-K lenses for a minimum of seven consecutive hours nightly over a period of 12 months. Follow-up visits occurred at the initiation of treatment, and then at 1 day, 1 week, 1 month, 3 months, 6 months, and 12 months after ortho-K treatment. During each visit, participants underwent slit lamp examinations to detect any contact-lens-related complications or adverse events. Ocular biological characteristics were assessed before treatment and at 1, 6, and 12 months post-treatment, using instruments such as the IOL-Master 700 (Carl Zeiss Meditec AG, Jena, Germany), corneal topography (Medmont E-300, Australia), and non-contact tonometer (NT-3000; NIDEK, Gamagori, Aichi, Japan). Quantitative choroidal parameters were assessed with spectral domain OCT (SD-OCT). Inspections were conducted at consistent times of the day (9:00 to 15:00) to minimize daily variations.

On the basis of reports indicating that AL increases by approximately 0.2 mm per year in patients wearing ortho-K lenses, and referencing studies that use a 0.2 mm per year increase to categorize slow or fast AL progression groups [5, 27–30], this study classified subjects after 1-year ortho-K treatment into two groups: slow AL progression (AL elongation ≤ 0.20 mm) and fast AL progression (AL elongation > 0.20 mm).

SD-OCT Image Acquisition

Data were acquired using the enhanced depth imaging mode of Spectralis OCT (Heidelberg Engineering, Heidelberg, Germany). A total of 31 grating scans, centered on the fovea with a scan range of 20 × 20 degrees (6 × 6 mm), were performed (Fig. 1). Each B-scan consisted of 768 A-scans in high-speed mode. To improve the signal-to-noise ratio, automatic real-time tracking was employed, averaging 30 frames per B-scan. This ensured that the OCT image sets obtained were of sufficient quality for choroidal segmentation. Baseline and 1-month follow-up OCT images were longitudinally captured at the same matched fundus locations using the follow-up mode of the instrument software.

Calculation of Choroidal Quantitative Parameters

Choroidal images were analyzed utilizing SD-OCT volumetric scan data, and quantitative parameters of the choroid were determined. Previous research by our group confirmed the effectiveness and reliability of the deep learning-based choroidal analysis model, successfully delineating the choroidal structural characteristics in children with myopia (Fig. 1). Our prior study detailed the model's principles and the formulas for calculating quantitative parameters [24]. Prior to calculating the quantitative choroidal parameters, the magnification of OCT images was adjusted on the basis of AL differences among subjects [31].

The Early Treatment Diabetic Retinopathy Study (ETDRS) grid is a standardized retinal segmentation system that divides the macular area into three concentric zones: the central subfield (1 mm), inner ring (3 mm), and outer ring (6 mm). Each zone is further subdivided into four quadrants (superior, inferior, nasal, temporal), resulting in nine distinct regions (Fig. 1a). The nine subfields include the central (C), superior inner ring (S13), inferior inner ring (I13), nasal inner ring (N13), temporal inner ring (T13), superior outer ring (S36),

inferior outer ring (I36), nasal outer ring (N36), and temporal outer ring subfield.

Mean values for choroidal volume, vascular volume (CVV), stromal volume (CSV), and CVI across the nine subfields of the ETDRS grid were calculated. Due to the resolution limitations of SD-OCT, distinguishing the small vessel layer (including small vessels and the choriocapillaris) was not feasible. Therefore, this study focused exclusively on calculating the quantitative choroidal parameters for the large-vessel choroidal layer (LVCL), medium-vessel choroidal layer (MVCL), and the total choroidal layer (TCL), which includes both LVCL and MVCL (Fig. 1). A comprehensive list of all abbreviations used in this manuscript and supplementary materials is provided in Supplementary Table S1.

Statistics

In this study, SER is defined as the sphere power plus half the negative cylinder power. Data from the right eye were selected for analysis, assuming symmetry between individual eyes. Statistical analysis was performed using SPSS Statistics software for Windows, version 23.0 (IBM, Armonk, NY, USA), and R version 4.3.2 (R Foundation for Statistical Computing). Unless specified otherwise, all values are presented as mean ± standard deviation. The Shapiro–Wilk test was initially applied to assess data normality. Differences in descriptive data were evaluated using the *t*-test, Mann–Whitney *U* test, or chi-squared test. Pearson's or Spearman's correlation analyses were conducted to assess the degree of association and statistical significance between variables. Stepwise multiple linear regression models were employed to identify factors associated with 1-year AL elongation. Factors with *P*-values less than 0.05 in univariate analyses were incorporated into the multivariate model, alongside age and gender as covariates.

To assess the predictive role of CVI, the predictive performance of the model for identifying children with slow or fast AL progression was assessed using the area under the receiver operating characteristic curve (AUC) derived from binary logistic regression analysis. The DeLong test was used to compare the differences between the AUCs of different models. On the basis of the final prediction model, a nomogram was constructed to visually depict the prediction outcomes. A two-sided *P*-value of less than 0.05 was considered statistically significant.

RESULTS

Table 1 presents the baseline characteristics of the cohort and delineates the differences between the slow AL progression group (AL elongation ≤ 0.20 mm) and the fast AL progression group (AL elongation > 0.20 mm). The mean age was 10.11 ± 1.78 years. Baseline measurements included intraocular pressure (16.14 ± 2.47 mmHg), central corneal thickness (555.73 ± 31.05 μm), SER (–2.45 ± 1.00 D), AL (24.54 ± 0.69 mm), anterior chamber depth (3.72 ± 0.19 mm), flat corneal keratometry (K1, 42.73 ± 1.25 D), steep K (K2, 43.89 ± 1.38 D), and average K (43.31 ± 1.30 D).

Participants exhibiting slow AL progression were significantly older than those with fast AL progression (10.59 ± 1.92 years versus 9.65 ± 1.52 years, $P < 0.001$). No significant differences were observed in baseline ocular biometrics and CVI between the two groups, with the exceptions of TCL_T13 ($P = 0.034$), TCL_N36 CVI ($P = 0.041$), and LVCL_T13 CVI ($P = 0.011$) (Table 2).

Changes of Ocular Biometrics and CVI after 1-Month Ortho-K Treatment

After 1 month of ortho-K treatment, all baseline ocular biometrics decreased significantly ($P < 0.001$) (Supplementary Table S2). No significant differences were observed in the 1-month changes in ocular biometrics between the two AL progression groups ($P > 0.390$) (Table 1). With the exception of the TCL_S36 subfield ($P = 0.070$), the 1-month CVI for both TCL and MVCL in all subfields was significantly lower than the baseline CVI ($P \leq 0.036$), with no significant differences observed in LVCL ($P > 0.05$).

The 1-month CVI changes in the slow AL progression group were significantly greater than those in the fast AL progression group for

Table 1 Demographics and ocular biometrics characteristics of the cohort

Characteristics	Total ($n = 257$)	Slow progression ≤ 0.20 mm ($n = 124$)	Fast progression > 0.20 mm ($n = 133$)	*P*-value
Demographics				
Age (years)	10.11 ± 1.78	10.59 ± 1.92	9.65 ± 1.52	**< 0.001**
Sex (male/female)	129/128	60/64	69/64	0.576
Baseline ocular biometrics				
IOP (mmHg)	16.14 ± 2.47	16.06 ± 2.50	16.21 ± 2.46	0.619
CCT (μm)	555.73 ± 31.05	553.98 ± 31.35	557.35 ± 30.78	0.386
SER (D)	−2.45 ± 1.00	−2.52 ± 1.01	−2.38 ± 0.98	0.246
AL (mm)	24.54 ± 0.69	24.57 ± 0.72	24.51 ± 0.66	0.511
ACD (mm)	3.72 ± 0.19	3.73 ± 0.21	3.70 ± 0.18	0.373
K1 (D)	42.73 ± 1.25	42.75 ± 1.28	42.70 ± 1.23	0.730
K2 (D)	43.89 ± 1.38	43.91 ± 1.40	43.88 ± 1.38	0.860
Average K (D)	43.31 ± 1.30	43.33 ± 1.40	43.29 ± 1.28	0.795
1-month changes of ocular biometrics				
IOP changes (mmHg)	−0.95 ± 2.07	−0.83 ± 2.00	−1.05 ± 2.13	0.391
CCT changes (μm)	−6.26 ± 7.88	−5.92 ± 7.34	−6.57 ± 8.37	0.509
K1 changes (D)	−2.04 ± 0.86	−2.03 ± 0.85	−2.05 ± 0.88	0.827
K2 changes (D)	−2.29 ± 0.99	−2.25 ± 1.01	−2.34 ± 0.98	0.462
Average K changes (D)	−2.17 ± 0.88	−2.14 ± 0.88	−2.19 ± 0.89	0.602
12-month changes of AL				
AL elongation (mm)	0.21 ± 0.17	0.08 ± 0.11	0.33 ± 0.11	**< 0.001**

Bold font indicates statistical significance

IOP intraocular pressure, *CCT* central corneal thickness, *SER* spherical equivalent refraction, *AL* axial length, *ACD* anterior chamber depth, *K* corneal keratometry, *K1* original flat K, *K2* original steep K

TCL_T36 ($P = 0.042$), LVCL_N36 ($P = 0.033$), and in all subfields of MVCL ($P < 0.006$) (Table 2).

Compared with baseline, 1-month choroidal volume and CSV showed significant increases across all choroidal sublayer subfields ($P < 0.030$), with the exception of the MVCL_C subfield ($P = 0.190$). CVV also saw significant increases in half of the choroidal sublayer subfields (14/27) (Supplementary Tables S3–5).

The Relationship between Ocular Biometrics, CVI, and 1-Year AL Elongation

After 1-year ortho-K treatment, the mean AL elongation across all participants was 0.21 ± 0.17 mm, with the slow AL progression group (0.08 ± 0.11 mm) showing significantly less elongation than the fast AL progression

Table 2 Baseline and 1-month changes in CVI of the cohort

	Baseline CVI (%)				1-month Changes of CVI (%)				
	Total ($n = 257$)	Slow progression ≤ 0.20 mm ($n = 124$)	Fast progression > 0.20 mm ($n = 133$)	*P*-value[a]	Total ($n = 257$)	Slow progression ≤ 0.20 mm ($n = 124$)	Fast progression > 0.20 mm ($n = 133$)	*P*-value[b]	*P*-value[c]
TCL_C	26.64 ± 4.01	26.75 ± 4.23	26.54 ± 3.80	0.676	−0.55 ± 3.52	−0.60 ± 3.48	−0.51 ± 3.58	0.841	**0.013**
TCL_S13	27.16 ± 3.22	27.16 ± 3.21	27.17 ± 3.25	0.979	−0.37 ± 2.79	−0.40 ± 2.78	−0.33 ± 2.81	0.832	**0.036**
TCL_I13	27.29 ± 3.27	27.23 ± 3.36	27.35 ± 3.20	0.766	−0.43 ± 2.60	−0.45 ± 2.51	−0.41 ± 2.68	0.895	**0.008**
TCL_T13	27.27 ± 2.93	26.87 ± 3.10	27.64 ± 2.71	**0.034**	−0.65 ± 2.62	−0.59 ± 2.70	−0.70 ± 2.56	0.730	**< 0.001**
TCL_N13	25.66 ± 3.25	25.46 ± 3.43	25.86 ± 3.07	0.325	−0.32 ± 2.41	−0.57 ± 2.34	−0.10 ± 2.45	0.118	**0.032**
TCL_S36	28.65 ± 2.50	28.54 ± 2.53	28.75 ± 2.47	0.497	−0.22 ± 1.93	−0.40 ± 1.91	−0.05 ± 1.94	0.144	0.070
TCL_I36	28.46 ± 2.46	28.20 ± 2.71	28.70 ± 2.18	0.109	−0.32 ± 1.86	−0.38 ± 1.71	−0.27 ± 1.98	0.638	**0.006**
TCL_T36	28.43 ± 2.41	28.26 ± 2.55	28.59 ± 2.27	0.268	−0.53 ± 1.81	−0.77 ± 1.88	−0.31 ± 1.73	**0.042**	**< 0.001**
TCL_N36	25.86 ± 3.04	25.46 ± 2.99	26.23 ± 3.06	**0.041**	−0.31 ± 1.94	−0.36 ± 1.95	−0.26 ± 1.94	0.671	**0.011**
LVCL_C	27.22 ± 5.04	27.40 ± 5.26	27.05 ± 4.83	0.573	−0.20 ± 4.92	−0.28 ± 4.91	−0.13 ± 4.94	0.808	0.516
LVCL_S13	27.59 ± 4.15	27.60 ± 4.21	27.58 ± 4.11	0.960	0.38 ± 3.75	0.39 ± 3.97	0.38 ± 3.55	0.987	0.103
LVCL_I13	27.51 ± 3.97	27.44 ± 4.22	27.58 ± 3.74	0.786	0.05 ± 3.59	0.02 ± 3.58	0.09 ± 3.62	0.878	0.811
LVCL_T13	27.56 ± 3.60	26.98 ± 3.76	28.11 ± 3.37	**0.011**	0.14 ± 3.54	0.19 ± 3.58	0.09 ± 3.53	0.832	0.538
LVCL_N13	26.23 ± 4.05	25.97 ± 4.28	26.47 ± 3.84	0.323	0.22 ± 3.46	0.45 ± 3.51	0.01 ± 3.41	0.314	0.299
LVCL_S36	29.90 ± 3.16	29.80 ± 3.19	29.98 ± 3.15	0.644	0.16 ± 2.53	0.15 ± 2.46	0.18 ± 2.61	0.915	0.300
LVCL_I36	29.43 ± 3.21	29.26 ± 3.52	29.59 ± 2.90	0.408	0.02 ± 2.39	0.08 ± 2.34	−0.04 ± 2.43	0.684	0.918
LVCL_T36	29.64 ± 2.96	29.46 ± 3.05	29.80 ± 2.88	0.358	−0.18 ± 2.35	−0.27 ± 2.55	−0.09 ± 2.16	0.539	0.227
LVCL_N36	26.00 ± 3.64	25.58 ± 3.49	26.40 ± 3.74	0.072	0.24 ± 2.75	0.62 ± 2.56	−0.11 ± 2.88	**0.033**	0.161
MVCL_C	24.96 ± 4.69	24.90 ± 4.75	25.03 ± 4.65	0.831	−1.74 ± 3.60	−2.61 ± 3.54	−0.93 ± 3.47	**< 0.001**	**< 0.001**
MVCL_S13	25.99 ± 4.30	25.88 ± 4.76	26.09 ± 3.84	0.698	−1.37 ± 2.86	−2.06 ± 2.82	−0.73 ± 2.75	**< 0.001**	**< 0.001**
MVCL_I13	26.66 ± 4.35	26.65 ± 4.22	26.68 ± 4.49	0.953	−1.38 ± 2.63	−2.26 ± 2.63	−0.57 ± 2.37	**< 0.001**	**< 0.001**
MVCL_T13	26.44 ± 4.03	26.51 ± 4.24	26.37 ± 3.83	0.787	−1.30 ± 2.77	−2.08 ± 2.64	−0.58 ± 2.69	**< 0.001**	**< 0.001**
MVCL_N13	24.16 ± 3.98	24.09 ± 4.25	24.23 ± 3.74	0.768	−1.06 ± 2.74	−1.75 ± 2.82	−0.42 ± 2.51	**< 0.001**	**< 0.001**
MVCL_S36	25.45 ± 3.79	25.21 ± 4.03	25.67 ± 3.55	0.332	−0.76 ± 2.17	−1.32 ± 2.10	−0.23 ± 2.10	**< 0.001**	**< 0.001**
MVCL_I36	26.00 ± 3.56	25.60 ± 3.68	26.38 ± 3.41	0.078	−1.09 ± 2.24	−1.64 ± 2.19	−0.58 ± 2.18	**< 0.001**	**< 0.001**
MVCL_T36	25.46 ± 3.24	25.26 ± 3.39	25.66 ± 3.11	0.327	−1.14 ± 2.14	−1.95 ± 2.12	−0.38 ± 1.87	**< 0.001**	**< 0.001**
MVCL_N36	25.52 ± 3.81	25.15 ± 4.08	25.87 ± 3.53	0.133	−0.46 ± 2.30	−0.88 ± 2.42	−0.08 ± 2.12	**0.005**	**< 0.001**

The nine subfields in ETDRS grid include central (C), superior inner ring (S13), inferior inner ring (I13), temporal inner ring (T13), nasal inner ring (N13), superior outer ring (S36), temporal outer ring (T36), inferior outer ring (I36), and nasal outer ring (N36). Bold font indicates statistical significance

CVI choroidal vascularity index, *TCL* total-vessel choroidal layer, *LVCL* large-vessel choroidal layer, *MVCL* medium-vessel choroidal layer

[a] *P*-value: Comparison of differences in baseline CVI between slow and fast progression groups

[b] *P*-value: Comparison of differences in 1-month changes of CVI between slow and fast progression groups

[c] *P*-value: Comparison of differences between baseline CVI and 1-month CVI

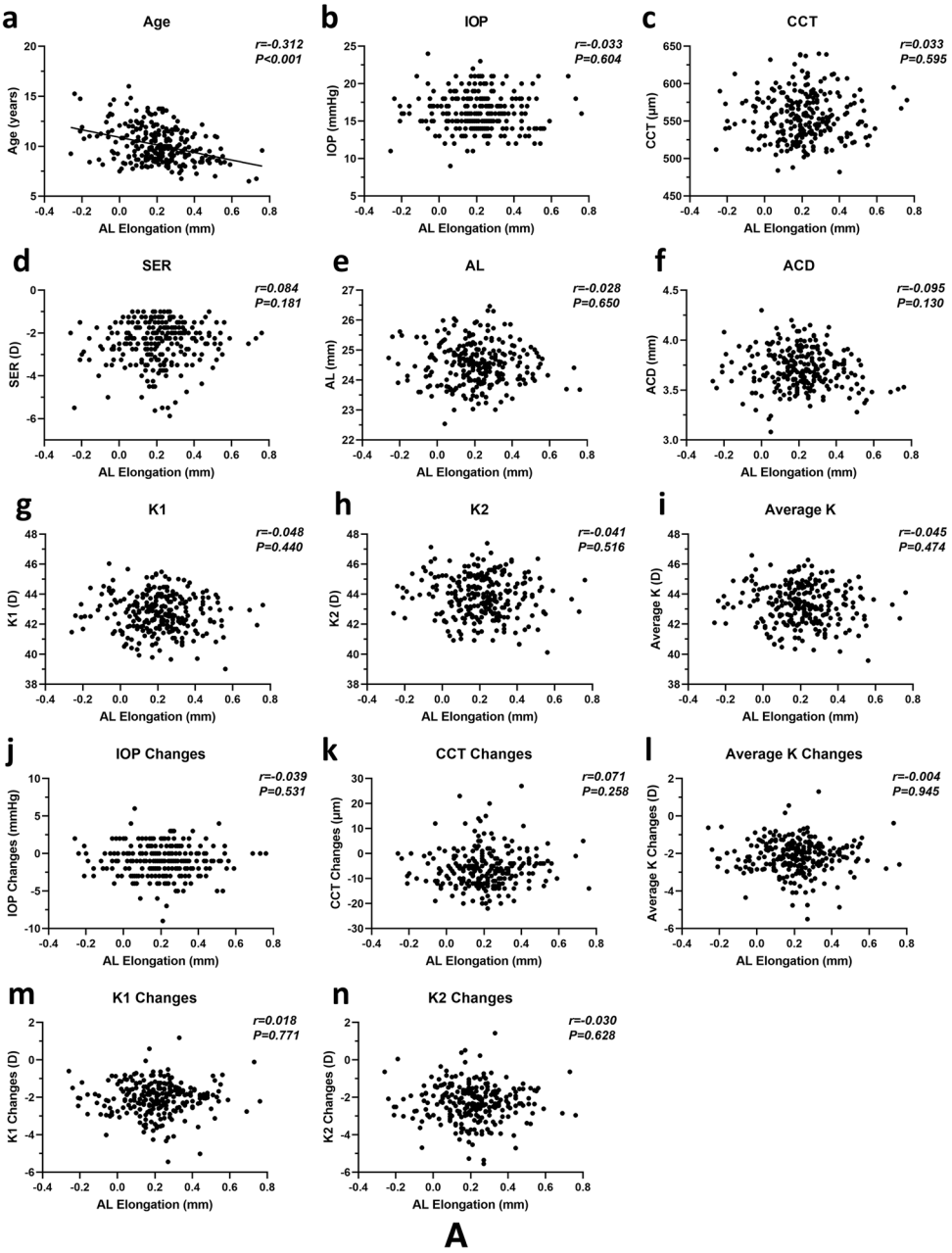


Fig. 2 Correlation of metrics at baseline and 1-month changes with 1-year AL elongation. The nine subfields in ETDRS grid include central (C), superior inner (S13), inferior inner (I13), temporal inner (T13), nasal inner (N13), superior outer (S36), temporal outer (T36), inferior outer (I36), and nasal outer (N36). **A** Correlation of ocular biometrics at baseline and 1-month changes with 1-year AL elongation. **B** Correlation of 1-month CVI changes of TCL with 1-year AL elongation. **C** Correlation of 1-month CVI changes of LVCL with 1-year AL elongation. **D** Correlation of 1-month CVI changes of MVCL with 1-year AL elongation. *AL* axial length, *IOP* intraocular pressure, *CCT* central corneal thickness, *SER* spherical equivalent refraction, *ACD* anterior chamber depth, *CVI* choroidal vascularity index, *TCL* total-vessel choroidal layer, *LVCL* large-vessel choroidal layer, *MVCL* medium-vessel choroidal layer

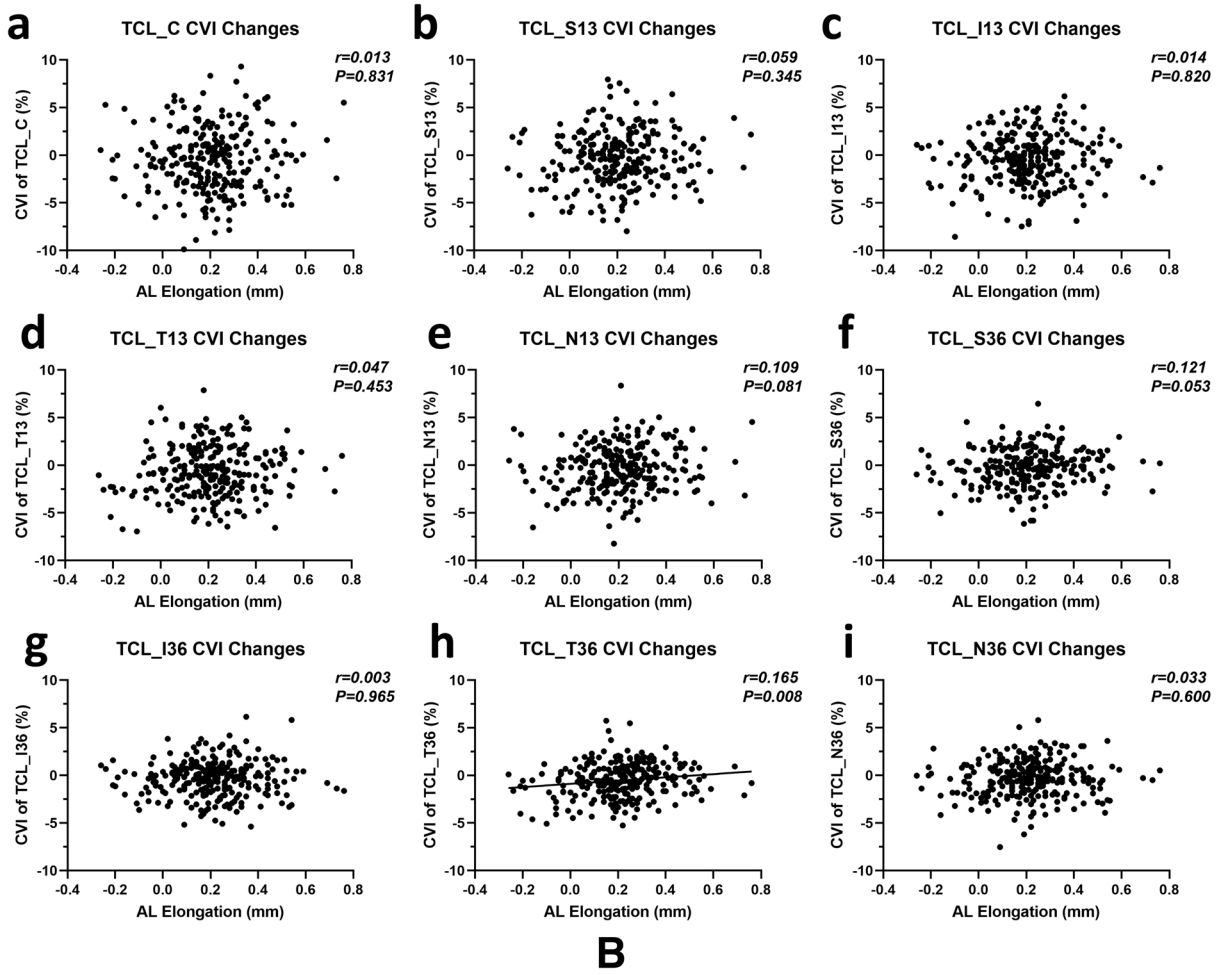


Fig. 2 continued

group (0.33 ± 0.11 mm) ($P < 0.001$) (Table 1). Figure 2 (A–D) presents scatterplots for baseline ocular biometrics, 1-month changes in ocular biometrics and CVI, and 1-year AL elongation. In terms of ocular biometrics, only baseline age showed a significant negative correlation with 1-year AL elongation ($r = -0.312$, $P < 0.001$).

Baseline Total_T13 CVI and 1-month CVI changes across all MVCL subfields were significantly positively correlated with 1-year AL elongation. The 1-month CVI changes showed no correlation with 1-year AL elongation across all TCL and LVCL subfields, with the exception of the Total_T36 subfield ($r = 0.165$, $P = 0.008$) (Fig. 2, Supplementary Table S6).

Multiple Linear Regression Analysis on the Factors Correlated with 1-Year AL Elongation

Utilizing statistically significant factors identified in the univariate analysis, a stepwise multiple linear regression analysis was conducted, resulting in a significantly adjusted model ($P < 0.001$, $R = 0.570$) (Supplementary Table S7). The model revealed that baseline TCL_T13 CVI ($\beta = 0.146$, $P = 0.006$) and 1-month CVI changes in the MVCL_T36 subfield ($\beta = 0.337$, $P < 0.001$) and MVCL_N13 subfield ($\beta = 0.174$, $P = 0.002$) served as independent predictors of 1-year AL elongation.

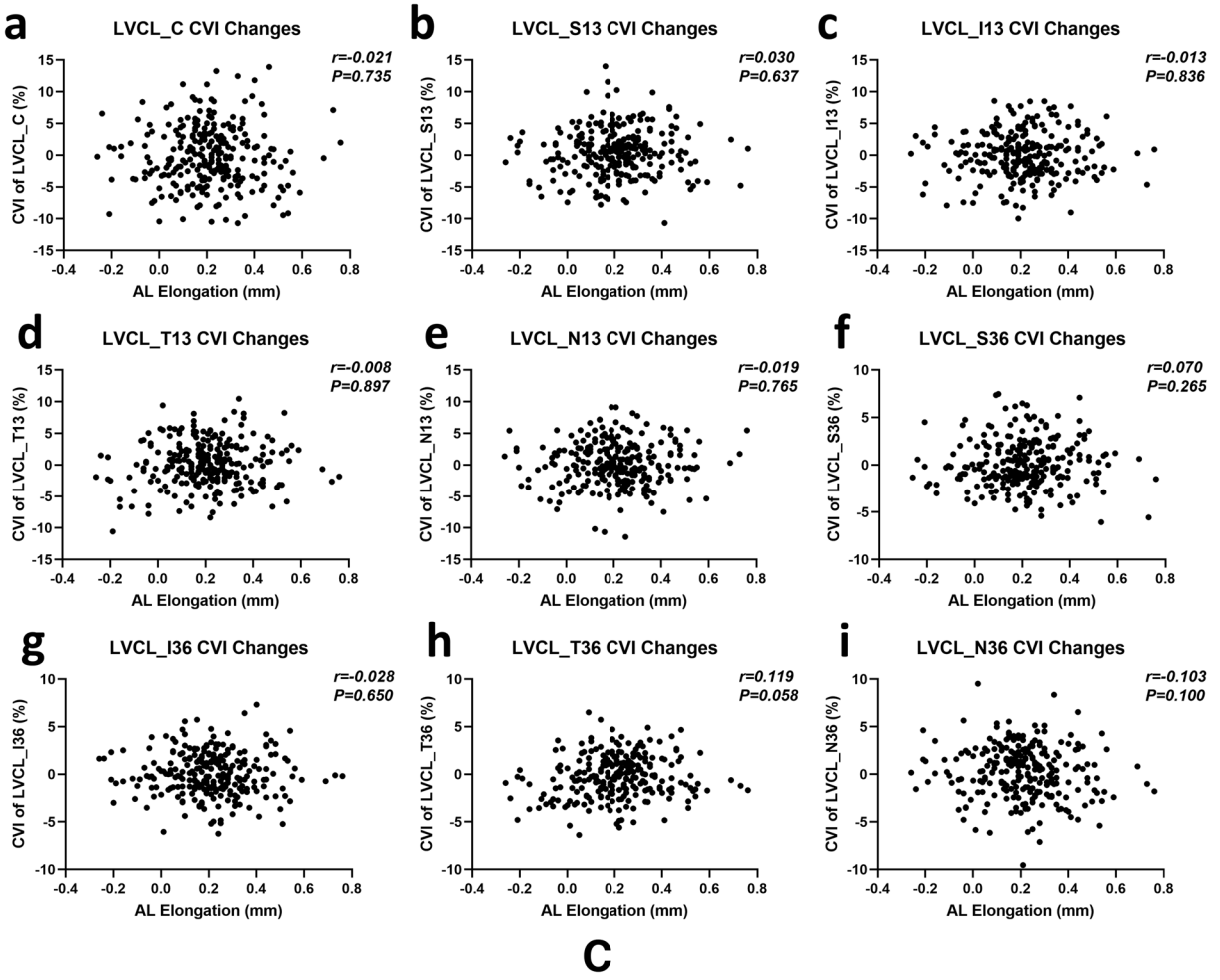


Fig. 2 continued

Figure 3 displays the AUC of the prediction model, utilizing CVI biomarkers to distinguish between slow and fast AL progression in children with myopia after 1-year of ortho-K treatment. AUC values for models constructed from independent influencing factors included: model 1 (0.574, 95% CI 0.503–0.644), model 2 (0.709, 95% CI 0.645–0.772), and model 3 (0.646, 95% CI 0.578–0.713). Given that the AUC value of model 2 was significantly higher than that of model 1, and no significant difference existed between model 3 and the other two models (Supplementary Table S8). Three factors were further combined to construct additional prediction models, namely models 4, 6, 8, and 10 (Fig. 3). No significant difference in AUC value was observed between model 2 (which solely includes 1-month CVI changes in MVCL_T36) and models 4, 6, 8, and 10. Model 3's AUC value (solely including 1-month CVI changes in MVCL_N13) was significantly lower compared with models 8 and 10 (both incorporating 1-month CVI changes in MVCL_T36).

Therefore, age and sex were incorporated into models containing the factor of 1-month CVI changes in MVCL_T36 (models 4, 8, and 10). AUC values for the models were as follows: model 5 (0.909, 95% CI 0.874–0.944), model 9 (0.905, 95% CI 0.870–0.941), and model 11 (0.909, 95% CI 0.875–0.944). The AUC values for these models were significantly higher than those before the addition of age and sex factors, with no significant differences in AUC observed among the three models. Consequently, two

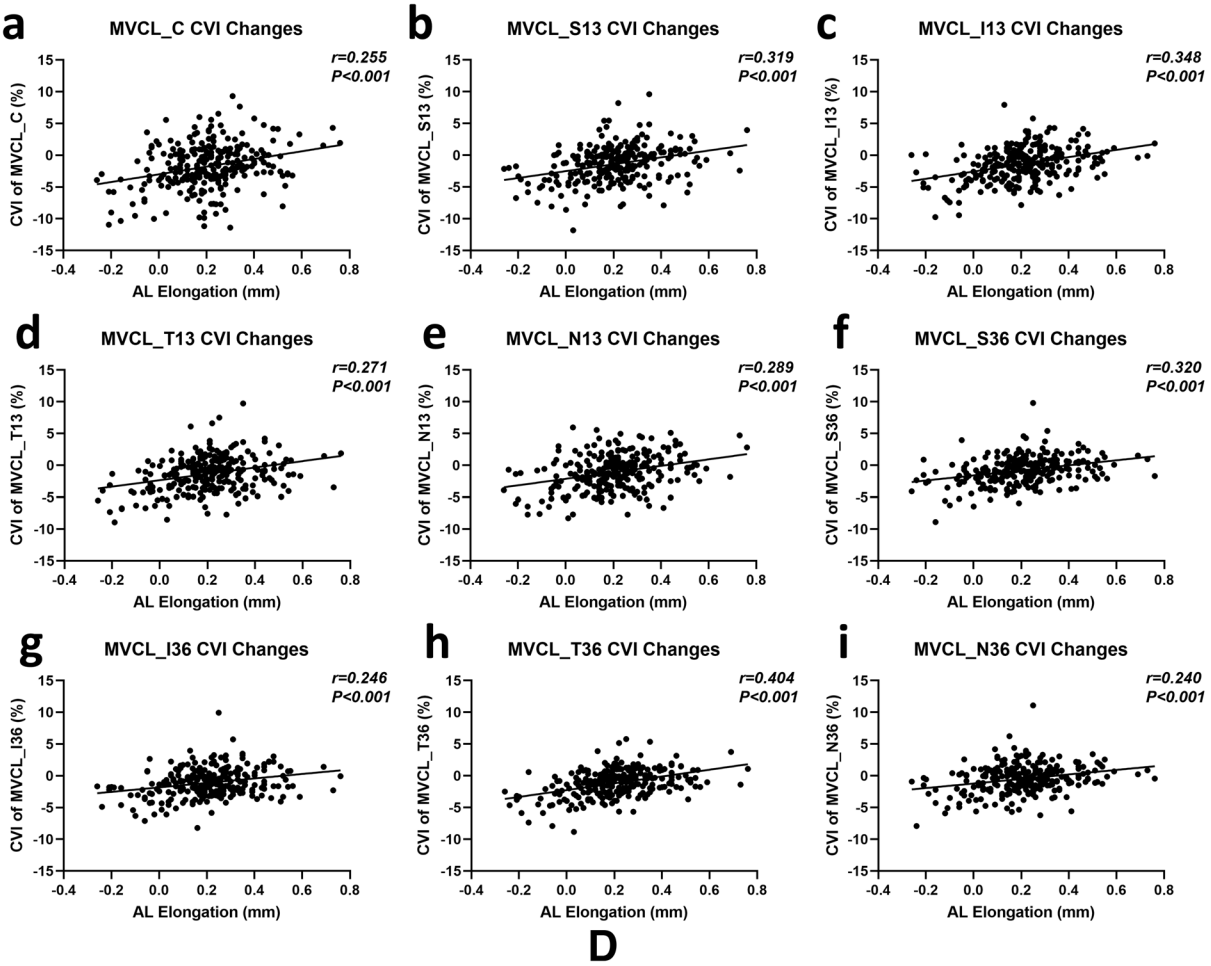


Fig. 2 continued

final models, model 5 and model 9, were constructed. For constructing model 9, only the 1-month CVI changes in MVCL were required. Thus, the final model, incorporating factors such as age, sex, and 1-month CVI changes in MVCL_T36 and MVCL_N13, was established, and a nomogram was created to predict slow or fast AL progression in ortho-K lens wearers (Supplementary Figure S1).

DISCUSSION

This study prospectively demonstrates that 1-month changes in CVI within the MVCL can effectively predict outcomes of ortho-K treatment. Firstly, it was observed that 1-month CVI across all subfields of TCL and MVCL were significantly lower than the baseline CVI (except for Total_S36), while no significant difference was observed in the LVCL. Disproportionate increases in CVV and CSV led to changes in CVI. Secondly, baseline CVI in TCL_T13, 1-month CVI changes in TCL_T36, and all subfields of MVCL were significantly positively correlated with AL elongation after 1-month ortho-K treatment. Finally, indicators independently related to AL elongation were identified: baseline TCL_T13 CVI, and short-term CVI changes in the MVCL_T36 and MVCL_N13 subfields. The model comprising 1-month CVI changes in the MVCL_T36 and MVCL_N13 subfields, age and gender, accurately predicts the fast AL

a

Model/Biomarkers	Total_T13	MVCL_T36 Changes	MVCL_N13 Changes	Age	Gender	AUC (95% CI)
Model 1	√					0.574 (0.503 to 0.644)
Model 2		√				0.709 (0.645 to 0.772)
Model 3			√			0.646 (0.578 to 0.713)
Model 4	√	√				0.723 (0.661 to 0.785)
Model 5	√	√		√	√	0.909 (0.874 to 0.944)
Model 6	√		√			0.661 (0.594 to 0.728)
Model 7	√		√	√	√	0.854 (0.809 to 0.899)
Model 8		√	√			0.717 (0.655 to 0.779)
Model 9		√	√	√	√	0.905 (0.870 to 0.941)
Model 10	√	√	√			0.736 (0.675 to 0.797)
Model 11	√	√	√	√	√	0.909 (0.875 to 0.944)

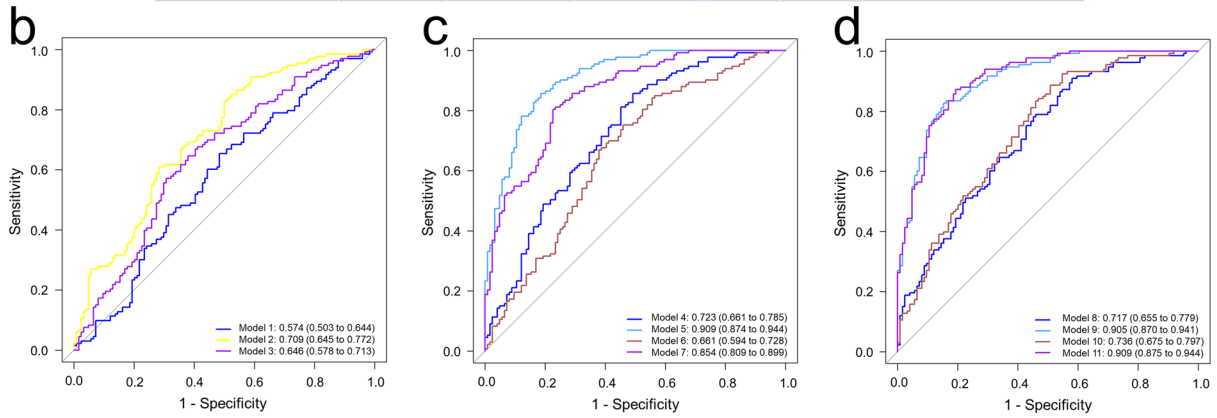


Fig. 3 ROC curves of the prediction models for discriminating slow and fast AL progression of children with myopia with 1-year ortho-K treatment. *ROC* receiver operating characteristic, *AL* axial length, *ortho-K* orthokeratology

progression group (AL change > 0.2 mm) and slow AL progression group (AL change ≤ 0.2 mm) after 1-year of ortho-K treatment.

Initial Age Significantly Correlated with AL elongation after Ortho-K Treatment

Previous studies have reported that AL elongation after ortho-K treatment was significantly correlated with baseline age [3–5, 7, 8, 32], changes in corneal refractive power and central corneal thickness [5, 7], and pupil diameter [33]. The research results regarding baseline SER and AL were contradictory. Several studies found no significant correlation between baseline AL or myopia degree and AL changes during ortho-K treatment [4, 5, 13, 14]. However, some studies observed that wearers of ortho-K lenses with a higher degree of myopia could achieve more effective myopia control [10–12]. Consistent with most published studies, this study identified a significant negative correlation between 1-year AL elongation and initial age in children with myopia wearing ortho-K lenses. That is, the younger the children with myopia, the greater the AL elongation observed after 1-year of ortho-K treatment. This pattern aligns with the natural progression of myopia in children. In younger children, both myopia progression and AL elongation occur more rapidly [14, 34]. In studies noting AL shortening following ortho-K treatment, subjects exhibiting AL shortening were typically young adults (25.62 ± 3.57 years old) or older children, with initial age demonstrating a significant correlation with AL shortening [28, 35–37]. These findings further substantiate the correlation between initial age and AL growth from another perspective.

This study did not find a correlation between baseline and 1-month changes of ocular biometrics and 1-year AL elongation. Given the conflicting results across studies and the diverse nature of ocular biometrics, the varying and complex changes in corneal topography induced by ortho-K lenses may offer one possible explanation [32]. It is well known that reduced central corneal refractive power and increased peripheral corneal refractive power after ortho-K treatment can lead to more peripheral retinal myopia defocusing [15]. Even among patients wearing the same brand of ortho-K lenses, differences in factors such as the size of the treatment area, and the amplitude and width of the central steepening, as well as the asphericity of the central flat area, can lead to variations in corneal topography and peripheral retinal defocus, thus influencing myopia control effectiveness. Previous studies have suggested that ortho-K lenses with smaller treatment areas and greater central steepness enhance myopia control effectiveness [38, 39]. Therefore, biological indicators that swiftly respond to peripheral retinal defocus and participate in myopia development are more apt as predictive markers for myopia control effectiveness.

The Potential Role of Choroidal Biometrics in Predicting the Effect of Myopia Control after Ortho-K Treatment

Multiple animal studies have demonstrated that the choroid can regulate its thickness, rapidly respond to retinal defocus, and transmit visual signals from the retina to the sclera, thus modulating eye growth and myopia progression [40, 41]. The choroidal response was remarkably swift, with observable thickness changes occurring within hours after defocus was applied. The primary anatomical change associated with increased thickness was the significant expansion of the choroidal cavity [41, 42]. Myopia development was accompanied by choroidal thinning and a decrease in choroidal blood flow. Conversely, during myopia recovery, the choroid thickened, resulting in a shift of the retina toward a new focal plane. Furthermore, a significant increase in choroidal blood flow preceded the increase in choroidal thickness and proved to be more transient than the latter. These findings suggest that increases in choroidal blood flow could trigger or potentially drive subsequent choroidal dilation [43]. Molecular signaling shifts induced by peripheral retinal myopic defocus after ortho-K lens wear led to alterations in choroidal thickness and blood flow, which may alleviate scleral hypoxia, facilitate remodeling, and delay axial length elongation [16].

An increasing number of studies have indicated changes in choroidal structure after ortho-K treatment. Several studies have reported significant choroidal thickening compared with the control group or baseline data after 3 weeks to 6 months of ortho-K treatment [16–19], and identified a significant correlation between short-term changes in choroidal thickness and AL changes [16, 18, 19]. However, choroidal thickness exhibited considerable variability, influenced by factors such as age, refractive error, axial length, intraocular pressure, systolic pressure, and choroidal lumen area [20, 21], and was also sensitive to segmentation errors [22]. In contrast to choroidal thickness, CVI demonstrated lower variability, improved reproducibility, and lacked significant associations with factors such as age, systolic blood pressure, AL, or intraocular pressure [23].

Previous studies have observed significant increases in choroidal thickness of the macular fovea and its temporal and nasal sides compared with baseline data after 6 months of ortho-K treatment [19]. During AL elongation and choroidal thinning, the peripheral retina experienced more pronounced choroidal thinning due to the higher metabolic demand in the central fovea [44]. Furthermore, animal experiments involving chicks and monkeys have demonstrated that peripheral myopic defocus reduces AL elongation [45, 46], particularly in the near peripheral region approximately 20° from the central fovea [47]. Therefore, it is essential to investigate the regional changes in the choroid around the macular fovea on a broader scale.

Compared with traditional studies using two-dimensional images (single B-scan images) to assess a limited area of the choroid, three-dimensional CVI covering a larger area of the fundus reveals the true state of the highly vascularized

choroid system more accurately, particularly the LVCL and MVCL [26]. Therefore, this study assessed three-dimensional CVI across a 6 mm diameter circular area in the fundus, aiding in evaluating choroidal vascular system changes post-ortho-K treatment and potentially predicting myopia control effectiveness.

Short-Term CVI Changes Significantly Correlated with 1-Year AL Elongation

In this study, baseline CVI in the TCL_T13 subfield, along with short-term CVI changes in MVCL_T36 and MVCL_N13 subfields, were independently associated with AL elongation. These findings suggest their potential utility in predicting rapid versus slow AL progression after 1-year ortho-K treatment. Previous studies have reported expansion of choroidal vascular-stromal structures after ortho-K treatment, with dynamic remodeling of the choroidal vasculature potentially underlying myopia control mechanisms [6, 25, 48, 49]. On the basis of these observations, we hypothesize that baseline CVI reflects the initial balance between the vascular and stromal components of the choroid, while subsequent choroidal vascular-stroma remodeling during ortho-K treatment may influence eye growth patterns.

After 1 month of ortho-K treatment, CVI in all TCL and MVCL subfields showed a significant decrease compared with baseline ($P \leq 0.036$), except for TCL_S36 subfield ($P = 0.070$). In contrast, no significant change was observed in the LVCL ($P > 0.05$). Further analyses revealed significant increases in choroidal volume and CSV in nearly all subfields except the central subfield, while CVV increased significantly in half of the subfields (14/27) following 1-month of ortho-K treatment (Supplementary Tables S3–S5). These results support our hypothesis that disproportionate increases in vascular and stromal components within TCL and MVCL drive the observed decline in CVI over 1 month. Notably, MVCL is primarily composed of medium-sized choroidal vessels that are crucial for local blood flow regulation and metabolic exchange [40]. The dynamic vascular-stroma remodeling observed may reflect ortho-K-induced optical defocus, which alters choroidal blood flow and consequently affects scleral remodeling mechanisms that govern AL elongation [16, 43, 50].

Additionally, studies have demonstrated regional differences in choroidal sensitivity to short-term optical defocus in humans [51, 52], potentially attributable to variations in autonomic innervation, nonvascular smooth muscle distribution, and region-specific choroidal blood flow [40]. This may partly explain why predictive biomarkers for AL elongation in our study were predominantly located in the nasal and temporal choroidal regions.

Wu et al. found that baseline CVI, rather than 1-month CVI changes, was significantly associated with 1-year AL elongation [6]. In this study, baseline CVI in the Total_T13 subfield and 1-month CVI changes in the TCL_T36 subfield, as well as all MVCL subfields, were significantly correlated with 1-year AL elongation. Wu et al. used horizontal B-scan images across the fovea and optic disc to analyze CVI, with the 6-mm macular region centered on the fovea as the region of interest. In this study, the ETDRS grid was used to partition the fundus, and the TCL, LVCL, and MVCL were analyzed. Therefore, variations in measurement methods, studied fundus areas, and choroidal sublayers may account for differences in research outcomes.

Additionally, a significant negative correlation was observed between 1-year AL elongation and 1-month changes in choroidal CVV (except for the TCL_T36 subfield), CSV, and choroidal volume across all ETDRS grid subfields of TCL. This mirrors the findings in Wu et al.'s study, demonstrating a significant negative correlation between 1-year eyeball elongation and monthly changes in luminal, stromal, and total choroidal area [6] (Supplementary Tables S9–11).

The Role of Short-Term MVCL CVI Changes in Predicting the Efficacy of Ortho-K Treatment

Reports indicate that ortho-K treatment reduces AL elongation in children with myopia by 32% to 63% over 2 years compared with monocular lenses treatment, with an average axial change ranging from 0.36 to 0.47 mm [5, 29, 30].

Multiple studies have shown that the annual average AL progression for subjects using ortho-K lenses ranged from 0.15 to 0.20 mm, in contrast to 0.28 to 0.39 mm in the control group [4, 10, 14, 15, 32]. Other reports indicate that patients wearing ortho-K lenses experienced an AL increase of approximately 0.2 mm/year, a rate that was used to define the slow and fast AL progression groups in this study [27, 28]. Accordingly, in this study, the group with annual AL elongation exceeding 0.2 mm was categorized as the fast AL progression group.

This study establishes a predictive model on the basis of short-term CVI changes in MVCL, demonstrating its potential role in identifying children with fast or slow AL progression after 1 year of ortho-K treatment. Independent factors influencing 1-year AL elongation were identified through stepwise multiple regression analysis, and various factors were combined to develop multiple predictive models for comparison. The results indicated that the AUC of the final model, established on the basis of MVCL_T36, MVCL_N13, age, and gender, could reach 0.905. This finding underscores the potential clinical application of short-term CVI changes in predicting the effectiveness of AL control during ortho-K treatment.

A significant advantage of this study is the utilization of an artificial intelligence-based choroidal automatic analysis model, which enables the analysis of choroidal sublayers and a larger fundus range of choroidal vascular structures. The three-dimensional CVI offers a superior evaluation of the state and changes within the choroidal vascular system. However, this study also presents some limitations. Notably, SD-OCT limits our investigation of the blood flow in the choriocapillaris. Swept-source OCTA holds greater promise for future research. Furthermore, the model developed in this study requires external validation, necessitating larger cohort studies in the future to ascertain the predictive model's performance.

CONCLUSIONS

Following ortho-K treatment, peripheral retinal myopic defocus may delay AL elongation, while the choroidal vascular system responds swiftly and undergoes structural changes. Increases in CVV and CSV are observable after 1 month of ortho-K treatment. A stable CVI, reflecting the ratio changes between CVV and CSV, can effectively predict long-term AL elongation in the early stages of ortho-K treatment. In the future, this predictive capability will enable clinicians to early detect the efficacy of ortho-K treatment in children with myopia and timely adjust treatment strategies.

ACKNOWLEDGEMENTS

We would like to thank the patients for their participation in this study.

Author Contributions. The authors were involved in the conception or design of the work (Junmeng Li, Bei Rong, Ruilin Zhu, Yanye Lu, Liu Yang), acquisition of data (Junmeng Li, Bei Rong, Xin Rong, Yuwei Wang, Yadi Zhang, Xiaopeng Gu), the analysis or interpretation of data (Junmeng Li, Lei Zhu, Shuang Zeng), drafting the work or revising it critically for important intellectual content (Junmeng Li, Bei Rong, Lei Zhu, Yanye Lu, Liu Yang), and final approval of the version to be published (Bei Rong, Ruilin Zhu, Xin Rong, Yuwei Wang, Yanye Lu, Liu Yang). All authors agree to be accountable for all aspects of the work, ensuring that any questions regarding the accuracy or integrity of any part of the work are appropriately investigated and resolved (Junmeng Li, Bei Rong, Lei Zhu, Ruilin Zhu, Xin Rong, Yuwei Wang, Yadi Zhang, Xiaopeng Gu, Shuang Zeng, Yanye Lu, Liu Yang). All authors read and approved the final manuscript.

Funding. Funding for this study, including the journal's rapid service fee, was from the National Natural Science Foundation of China, 82371064, Liu Yang, 82171059, Liu Yang, Peking University Health Science Center-Michigan Medicine Joint Institute for Translational and Clinical Research Discovery Awards, BMU2020JI006, Liu Yang.

Data Availability. The datasets utilized in this study are not publicly available due to reasonable privacy and security concerns. Limited access to the dataset can be made by request to the corresponding author.

Declarations

Conflict of Interest. Junmeng Li, Bei Rong, Lei Zhu, Ruilin Zhu, Xin Rong, Yuwei Wang, Yadi Zhang, Xiaopeng Gu, Shuang Zeng, Yanye Lu, and Liu Yang have nothing to disclose.

Ethical Approval. This study was conducted in accordance with the principles of the Declaration of Helsinki and received approval from the Ethics Committee of Peking University First Hospital Ethics Committee (approval no.: 2022-KY-190-001). Informed consent was obtained from all participants for the use of their data in this research.

Open Access. This article is licensed under a Creative Commons Attribution-NonCommercial 4.0 International License, which permits any non-commercial use, sharing, adaptation, distribution and reproduction in any medium or format, as long as you give appropriate credit to the original author(s) and the source, provide a link to the Creative Commons licence, and indicate if changes were made. The images or other third party material in this article are included in the article's Creative Commons licence, unless indicated otherwise in a credit line to the material. If material is not included in the article's Creative Commons licence and your intended use is not permitted by statutory regulation or exceeds the permitted use, you will need to obtain permission directly from the copyright holder. To view a copy of this licence, visit http://creativecommons.org/licenses/by-nc/4.0/.

REFERENCES

1. Holden BA, Fricke TR, Wilson DA, Jong M, Naidoo KS, Sankaridurg P, et al. Global prevalence of myopia and high myopia and temporal trends from 2000 through 2050. Ophthalmology. 2016;123:1036–42.
2. Saw S-M, Gazzard G, Shih-Yen EC, Chua W-H. Myopia and associated pathological complications. Ophthalmic Physiol Opt. 2005;25:381–91.
3. Zhu M-J, Feng H-Y, He X-G, Zou H-D, Zhu J-F. The control effect of orthokeratology on axial length elongation in Chinese children with myopia. BMC Ophthalmol. 2014;14:141.
4. Chen C, Cheung SW, Cho P. Myopia control using toric orthokeratology (TO-SEE study). Invest Ophthalmol Vis Sci. 2013;54:6510–7.
5. Cho P, Cheung S-W. Retardation of myopia in orthokeratology (ROMIO) study: a 2-year randomized clinical trial. Invest Ophthalmol Vis Sci. 2012;53:7077–85.
6. Wu H, Peng T, Zhou W, Huang Z, Li H, Wang T, et al. Choroidal vasculature act as predictive biomarkers of long-term ocular elongation in myopic children treated with orthokeratology: a prospective cohort study. Eye Vis (Lond). 2023;10:27.
7. Lee EJ, Lim DH, Chung T-Y, Hyun J, Han J. Association of axial length growth and topographic change in orthokeratology. Eye Contact Lens. 2018;44:292–8.
8. Zhong Y, Chen Z, Xue F, Miao H, Zhou X. Central and peripheral corneal power change in myopic orthokeratology and its relationship with 2-year axial length change. Invest Ophthalmol Vis Sci. 2015;56:4514–9.
9. Santodomingo-Rubido J, Villa-Collar C, Gilmartin B, Gutiérrez-Ortega R. Factors preventing myopia progression with orthokeratology correction. Optom Vis Sci. 2013;90:1225–36.
10. Lin W, Li N, Lu K, Li Z, Zhuo X, Wei R. The relationship between baseline axial length and axial elongation in myopic children undergoing orthokeratology. Ophthalmic Physiol Opt. 2023;43:122–31.
11. Wang B, Naidu RK, Qu X. Factors related to axial length elongation and myopia progression in orthokeratology practice. PLoS ONE. 2017;12:e0175913.
12. Kakita T, Hiraoka T, Oshika T. Influence of overnight orthokeratology on axial elongation in childhood myopia. Invest Ophthalmol Vis Sci. 2011;52:2170–4.
13. Santodomingo-Rubido J, Villa-Collar C, Gilmartin B, Gutiérrez-Ortega R, Sugimoto K. Long-term efficacy of orthokeratology contact lens wear in controlling the progression of childhood myopia. Curr Eye Res. 2017;42:713–20.

14. Hyman L, Gwiazda J, Hussein M, Norton TT, Wang Y, Marsh-Tootle W, et al. Relationship of age, sex, and ethnicity with myopia progression and axial elongation in the correction of myopia evaluation trial. Arch Ophthalmol. 2005;123:977–87.

15. Qi Y, Liu L, Li Y, Zhang F. Factors associated with faster axial elongation after orthokeratology treatment. BMC Ophthalmol. 2022;22:62.

16. Li Z, Hu Y, Cui D, Long W, He M, Yang X. Change in subfoveal choroidal thickness secondary to orthokeratology and its cessation: a predictor for the change in axial length. Acta Ophthalmol. 2019;97:e454–9.

17. Li Z, Cui D, Hu Y, Ao S, Zeng J, Yang X. Choroidal thickness and axial length changes in myopic children treated with orthokeratology. Cont Lens Anterior Eye. 2017;40:417–23.

18. Jin W-Q, Huang S-H, Jiang J, Mao X-J, Shen M-X, Lian Y. Short term effect of choroid thickness in the horizontal meridian detected by spectral domain optical coherence tomography in myopic children after orthokeratology. Int J Ophthalmol. 2018;11:991–6.

19. Wang Z, Chen J, Kang J, Niu T, Guo L, Fan L. Axial length control is associated with a choroidal thickness increase in myopic adolescents after orthokeratology. Eye Contact Lens. 2023;49:512–20.

20. Betzler BK, Ding J, Wei X, Lee JM, Grewal DS, Fekrat S, et al. Choroidal vascularity index: a step towards software as a medical device. Br J Ophthalmol. 2022;106:149–55.

21. Agrawal R, Ding J, Sen P, Rousselot A, Chan A, Nivison-Smith L, et al. Exploring choroidal angioarchitecture in health and disease using choroidal vascularity index. Prog Retin Eye Res. 2020;77:100829.

22. Zhao M, Alonso-Caneiro D, Lee R, Cheong AMY, Yu W-Y, Wong H-Y, et al. Comparison of choroidal thickness measurements using semiautomated and manual segmentation methods. Optom Vis Sci. 2020;97:121–7.

23. Agrawal R, Gupta P, Tan K-A, Cheung CMG, Wong T-Y, Cheng C-Y. Choroidal vascularity index as a measure of vascular status of the choroid: measurements in healthy eyes from a population-based study. Sci Rep. 2016;6:21090.

24. Li J, Zhu L, Zhu R, Lu Y, Rong X, Zhang Y, et al. Automated analysis of choroidal sublayer morphologic features in myopic children using EDI-OCT by deep learning. Transl Vis Sci Technol. 2021;10:12.

25. Zhu Q, Zhao Q. Short-term effect of orthokeratology lens wear on choroidal blood flow in children with low and moderate myopia. Sci Rep. 2022;12:17653.

26. Yang J, Wang E, Yuan M, Chen Y. Three-dimensional choroidal vascularity index in acute central serous chorioretinopathy using swept-source optical coherence tomography. Graefes Arch Clin Exp Ophthalmol. 2020;258:241–7.

27. Li X, Hu J, Peng Z, Chen S, Sun L, Wang K, et al. Association between choriocapillaris perfusion and axial elongation in children using defocus incorporated multiple segments (DIMS) spectacle lenses. Eye (Lond). 2023;37:3847–53.

28. Tang T, Li X, Chen S, Xu Q, Zhao H, Wang K, et al. Long-term follow-up of changes in ocular biometric parameters in orthokeratology lens wearers with relatively large-scale axial length reduction. Eye Vis (Lond). 2023;10:6.

29. Santodomingo-Rubido J, Villa-Collar C, Gilmartin B, Gutiérrez-Ortega R. Myopia control with orthokeratology contact lenses in Spain: refractive and biometric changes. Invest Ophthalmol Vis Sci. 2012;53:5060–5.

30. Hiraoka T. Myopia control with orthokeratology: a review. Eye Contact Lens. 2022;48:100–4.

31. Dai Y, Xin C, Zhang Q, Chu Z, Zhou H, Zhou X, et al. Impact of ocular magnification on retinal and choriocapillaris blood flow quantification in myopia with swept-source optical coherence tomography angiography. Quant Imaging Med Surg. 2021;11:948–56.

32. Holmes M, Liu M, Singh S. Retrospective analysis of axial length changes in overnight orthokeratology in an academic myopia control clinic. Optom Vis Sci. 2023;100:597–605.

33. Chen Z, Niu L, Xue F, Qu X, Zhou Z, Zhou X, et al. Impact of pupil diameter on axial growth in orthokeratology. Optom Vis Sci. 2012;89:1636–40.

34. Saw SM, Chua WH, Gazzard G, Koh D, Tan DTH, Stone RA. Eye growth changes in myopic children in Singapore. Br J Ophthalmol. 2005;89:1489–94.

35. Swarbrick HA, Alharbi A, Watt K, Lum E, Kang P. Myopia control during orthokeratology lens wear in children using a novel study design. Ophthalmology. 2015;122:620–30.

36. González-Mesa A, Villa-Collar C, Lorente-Velázquez A, Nieto-Bona A. Anterior segment changes produced in response to long-term overnight orthokeratology. Curr Eye Res. 2013;38:862–70.

37. Hu Y, Ding X, Jiang J, Yu M, Chen L, Zhai Z, et al. Long-term axial length shortening in myopic orthokeratology: incident probability, time course, and influencing factors. Invest Ophthalmol Vis Sci. 2023;64:37.

38. Pauné J, Fonts S, Rodríguez L, Queirós A. The role of back optic zone diameter in myopia control with orthokeratology lenses. J Clin Med. 2021;10:336.

39. Guo B, Cheung SW, Kojima R, Cho P. One-year results of the Variation of Orthokeratology Lens Treatment Zone (VOLTZ) study: a prospective randomised clinical trial. Ophthalmic Physiol Opt. 2021;41:702–14.

40. Nickla DL, Wallman J. The multifunctional choroid. Prog Retin Eye Res. 2010;29:144–68.

41. Wallman J, Wildsoet C, Xu A, Gottlieb MD, Nickla DL, Marran L, et al. Moving the retina: choroidal modulation of refractive state. Vision Res. 1995;35:37–50.

42. Nickla DL. Transient increases in choroidal thickness are consistently associated with brief daily visual stimuli that inhibit ocular growth in chicks. Exp Eye Res. 2007;84:951–9.

43. Zhang S, Zhang G, Zhou X, Xu R, Wang S, Guan Z, et al. Changes in choroidal thickness and choroidal blood perfusion in guinea pig myopia. Invest Ophthalmol Vis Sci. 2019;60:3074–83.

44. Tian F, Zheng D, Zhang J, Liu L, Duan J, Guo Y, et al. Choroidal and retinal thickness and axial eye elongation in Chinese junior students. Invest Ophthalmol Vis Sci. 2021;62:26.

45. Liu Y, Wildsoet C. The effect of two-zone concentric bifocal spectacle lenses on refractive error development and eye growth in young chicks. Invest Ophthalmol Vis Sci. 2011;52:1078–86.

46. Liu Y, Wildsoet C. The effective add inherent in 2-zone negative lenses inhibits eye growth in myopic young chicks. Invest Ophthalmol Vis Sci. 2012;53:5085–93.

47. Smith Iii EL, Arumugam B, Hung L-F, She Z, Beach K, Sankaridurg P. Eccentricity-dependent effects of simultaneous competing defocus on emmetropization in infant rhesus monkeys. Vision Res. 2020;177:32–40.

48. Liu M, Huang J, Xie Z, Wang Y, Wang P, Xia R, et al. Dynamic changes of choroidal vasculature and its association with myopia control efficacy in children during 1-year orthokeratology treatment. Cont Lens Anterior Eye. 2025;48: 102314.

49. Xu S, Wang Y, Ruan Z, Wang S, Yin R, Tang X, et al. Longitudinal changes in choroidal structures among children with low to moderate myopia under orthokeratology treatment. Cont Lens Anterior Eye. 2025;48: 102342.

50. Wu H, Chen W, Zhao F, Zhou Q, Reinach PS, Deng L, et al. Scleral hypoxia is a target for myopia control. Proc Natl Acad Sci U S A. 2018;115:E7091–100.

51. Hoseini-Yazdi H, Vincent SJ, Collins MJ, Read SA. Regional alterations in human choroidal thickness in response to short-term monocular hemifield myopic defocus. Ophthalmic Physiol Opt. 2019;39:172–82.

52. Moderiano D, Do M, Hobbs S, Lam V, Sarin S, Alonso-Caneiro D, et al. Influence of the time of day on axial length and choroidal thickness changes to hyperopic and myopic defocus in human eyes. Exp Eye Res. 2019;182:125–36.